



Cloud droplet size distribution broadening during diffusional growth: ripening amplified by deactivation and reactivation

Fan Yang¹, Pavlos Kollias^{1,2}, Raymond A. Shaw³, and Andrew M. Vogelmann¹

¹Brookhaven National Laboratory, Upton, New York, USA.

²Stony Brook University, Stony Brook, New York, USA.

³Michigan Technological University, Houghton, Michigan, USA.

Correspondence to: Fan Yang (fanyang@bnl.gov)

Abstract. Cloud droplet size distributions (CDSs), which are related to cloud albedo and lifetime, are usually broader in warm clouds than predicted from adiabatic parcel calculations. We investigate a mechanism for the CDS broadening using a Lagrangian bin-microphysics cloud parcel model that considers the condensational growth of cloud droplets formed on polydisperse, sub-micrometer aerosols in an adiabatic cloud parcel that undergoes vertical oscillations, such as those due to cloud circulations or turbulence. Results show that the CDS can be broadened during condensational growth as a result of Ostwald ripening amplified by droplet deactivation and reactivation, which is consistent with Korolev (1995). The relative roles of the solute effect, curvature effect, deactivation and reactivation on CDS broadening are investigated. Deactivation of smaller cloud droplets, which is due to the combination of curvature and solute effects in the downdraft region, enhances the growth of larger cloud droplets and thus contributes particles to the larger size end of the CDS. Droplet reactivation, which occurs in the updraft region, contributes particles to the smaller size end of the CDS. In addition, we find that growth of the largest cloud droplets strongly depends on the residence time of cloud droplet in the cloud rather than the magnitude of local variability in the supersaturation fluctuation. This is because the environmental saturation ratio is strongly buffered by smaller cloud droplets. Two necessary conditions for this CDS broadening, which generally occur in the atmosphere, are: (1) droplets form on polydisperse aerosols of varying hygroscopicity and (2) the cloud parcel experiences upwards and downwards motions. Therefore we expect that this mechanism for CDS broadening is possible in real clouds. Our results also suggest it is important to consider both curvature and solute effects before and after cloud droplet activation in a cloud model. The importance of this mechanism compared with other mechanisms on cloud properties should be investigated through in-situ measurements and 3-D dynamic models.

1 Introduction

Warm clouds play a crucial role in water cycle and energy balance on Earth (Boucher et al., 2013) so understanding the whole life cycle of warm cloud, including formation, development and precipitation, is important for better prediction of local weather and global climate. Cloud droplet growth is dominated by diffusion of water vapor at the early stage of cloud development, while collisional growth is believed to be the most important mechanism for drizzle formation and warm cloud precipitation (Pruppacher et al., 1998). Imaging an initially sub-saturated air parcel rising adiabatically, cloud forms at the lifting conden-



sation level and the growth of cloud droplets due to diffusional growth can be accurately predicted if we know the aerosol chemical composition. Because the linear growth rate of a cloud droplet is inversely proportional to droplet size, diffusional growth is inefficient when the droplet diameter is larger than $20 \mu\text{m}$ while collisional growth is efficient when the droplet diameter is larger than $38 \mu\text{m}$ (Hocking, 1959). In addition, the sizes of the smaller cloud droplets will approach those of the larger droplets and narrow the cloud droplet size distribution (CDS), which is also unfavorable for collisional growth (Mordy, 1959). If only diffusional growth is considered, several tens of minutes even up to hours will be needed for a cloud droplet to reach efficient-collision size in an ascending cloud parcel, which is much longer than the timescale typically observed (Laird et al., 2000).

The concept of a cloud parcel rising adiabatically in the atmosphere has been used to study cloud microphysical properties for decades. It is well known that the CDS becomes narrower if the cloud parcel rises adiabatically and only diffusional growth is considered. However, the CDS in a real cloud is usually wider than predicted by an adiabatic cloud parcel model and drizzle-size cloud droplets are frequently observed in warm clouds (e.g., Siebert and Shaw, 2017). An interesting question is to explain why the CDS is wider than predicted and the presence of the large droplet sizes in the tail of the distribution (e.g., Siebert and Shaw, 2017), which might be related to the fast-rain process in the atmosphere (e.g., Göke et al., 2007). Several possible mechanisms have been proposed, including the existence of giant cloud condensational nuclei (GCCN, usually defined as aerosols with dry diameter larger than few μm) (e.g., Feingold et al., 1999; Yin et al., 2000; Jensen and Lee, 2008; Cheng et al., 2009; Jensen and Nugent, 2017), lucky cloud droplets (e.g., Kostinski and Shaw, 2005; Naumann and Seifert, 2015; Lozar and Muessle, 2016), mixing with environmental air (e.g., Lasher-Trapp et al., 2005; Cooper et al., 2013; Korolev et al., 2013; Yang et al., 2016), supersaturation fluctuations (e.g., Chandrakar et al., 2016; Siebert and Shaw, 2017), and enhancement of collision efficiency due to turbulence or charge (e.g., Paluch, 1970; Grabowski and Wang, 2013; Falkovich and Pumir, 2015; Lu and Shaw, 2015). Recently, Jensen and Nugent (2017) investigated the effect of GCCN on droplet growth and rain formation using a cloud parcel model. They found that GCCN not only provides an embryo for big droplets at the activation stage, but also enhances droplet growth after activation due to the solute effect. For example, droplets formed on GCCN can still grow through condensation of water vapor in the downdraft region, even though the environment is subsaturated with respect to pure water (Jensen and Nugent, 2017). In fact, this is one example of irreversibility of droplet size spectrum shape during condensation growth due to solute and curvature effects (Korolev, 1995). Korolev (1995) analytically explained why irreversibility occurs in an environment experiencing supersaturation fluctuations if solute and curvature effects are considered. This irreversibility will promote the growth of large cloud droplets, lead to evaporation or even deactivation of small cloud droplets, and thus broaden the CDS.

Here we consider an adiabatic cloud parcel that experiences vertical oscillations, with cloud droplets that are formed on polydisperse, sub-micrometer aerosols. Results show that the CDS is broadened during diffusional growth due to Ostwald ripening and associated droplet deactivation and reactivation, which is consistent with Korolev (1995). In this study, we investigate (1) what are the relative roles of the solute and curvature effects on CDS broadening, and (2) what other factors can



affect this broadening? This paper is organized as follows. Section 2 introduces the basic setup for cloud parcel model, which is similar to Jensen and Nugent (2017) except that there are no GCCN. Results related to CDSB broadening and the associated sensitivities studies are detailed in Section 3. Conclusions are summarized in Section 4, including a discussion of implications in cloud observations and modeling.

5

2 Methods

A cloud parcel model with bin microphysics was used to conduct this study. The original version of the model was designed to study the warm cloud processes by Feingold et al. (1998) and since has been modified and applied to investigate various of microphysical problems (e.g., Feingold and Kreidenweis, 2000; Xue and Feingold, 2004; Ervens and Feingold, 2012; Yang et al., 2012; Li et al., 2013; Yang et al., 2016). In this study, the parcel starts rising at about 300 m below cloud base and starts descending at about 300 m above cloud base, which is similar to Jensen and Nugent (2017), except that our cloud parcel then experiences upward and downward oscillations between 50 m above cloud base and 300 m above cloud base (see Figure 1a). The ascending and descending velocities are set to be 0.5 m s^{-1} and -0.5 m s^{-1} for the control case. At the parcel's initial altitude of 600 m, the initial air temperature is 284.3 K, pressure is 938.5 hPa, and saturation ratio is 0.856, which are as same as Jensen and Nugent (2017).

The initial dry aerosols are ammonium sulphate with a log-normal size distribution range of 10 nm to 500 nm in radius. The sub-micrometer aerosols are parsed into 100 bins. The median radius is 50 nm with a geometric standard deviation of 1.4. The total number mixing ratio is 1000 mg^{-1} for the control case, which is about 1000 cm^{-3} (see Figure 1b). The model first calculates the equilibrium size of haze droplets for each bin at 85.6% relative humidity, as does Jensen and Nugent (2017). The curvature and solute effects are both considered during the growth process for each bin. The solute effect in droplet growth is calculated as a function of the molality of ammonium sulphate (Low, 1969). It should be noted that there are several methods to calculate the solute effect with the relative deviations for activation ranging up to 20%, but the differences are small for droplet growth (Heintzenberg et al., 2009). The total simulation time is 3 hours, and variables are recorded every 1 s that include temperature, pressure, height, water vapor mixing ratio, as well as droplet size and number concentration for each bin.

3 Results and discussions

3.1 Cloud droplet size distribution broadening

For the control case, the liquid water mixing ratio increases linearly with height in the ascending branches and decreases in the descending branches as shown in Figure 2a. Liquid water mixing ratio in the ascending branch is slightly smaller than that in the descending branch at the same height. The saturation ratio has an increasing trend in the ascending branch after each cycle,

30



but has a decreasing trend in the descending branch (indicated by red and blue arrows in Figure 2b). Droplet size as a function of height in two bins are shown in Figure 2c. The solid line is for the cloud droplet that formed on a dry aerosol of 503 nm and represents the largest droplet in our simulation. It grows in the ascending branch but it evaporates in the descending branch. Also, the droplet size for this bin increases after each cycle. The dashed line in Figure 2c is for the cloud droplet that formed on a dry aerosol of 51 nm. For this cloud droplet, the changes in radius with height are similar for the initial few cycles, after which the droplet totally evaporates. Ultimately, the aerosol is reactivated again as a cloud droplet by the end of the simulation (green dashed line). Thus the CDS broadens after each cycle as the larger droplets become larger and the smaller droplets either remain similarly sized or become smaller (see Figure 2d). All these features are consistent with Korolev (1995) (see Fig. 5 in his paper).

10

Korolev (1995) analytically investigate the narrowing and broadening of cloud droplet size distribution during condensation when solute and curvature effects are considered. He considers a cloud parcel oscillating vertically in simple harmonic motion. Results show that the CDS is irreversible if solute and curvature effects are considered. Irreversibility of the CDS will not only promote the growth of large droplets, but it will also lead to the evaporation, or even deactivation of small cloud droplets, and thus broaden the CDS. However, the relative roles of the solute effect, curvature effect, deactivation and reactivation on the broadening of droplet size distributions have not been investigated.

15

To explore the relative roles of different factors in this CDS broadening mechanism, three more cases are tested here. For the first case, we turn off both the solute and curvature effects for all cloud droplets after 700 s; this is the time when the cloud parcel first reaches 50 m above cloud base and is just below the oscillation layer. The result is shown in Figure 3a. For this case, the CDS repeats for each cycle, consistent with Korolev et al. (2013), and the total cloud droplet number concentration (n) is constant (red solid line in Figure 3d). For the second case, we only turn off the curvature effect but retain the solute effect. The result in Figure 3b shows that the largest droplet (with the most solute) can grow after each cycle while the smallest droplet size (with the least solute amount) does not change much after each cycle. However the size that largest droplet can reach is much smaller than that in the control case. Because the saturated water vapor pressure over a droplet formed on larger aerosol is lower than that formed on smaller aerosol due to the solute effect, the larger droplet grows faster than the smaller droplet in the updraft region, and it evaporates slower in the downdraft region. For this case, the solute effect alone cannot explain the larger cloud droplets in the control case. In addition, n is also a constant and droplet deactivation does not occur (green dashed line in Figure 3d). In the third case, we consider both curvature and solute effects, but we do not allow droplet reactivation. This means that once the droplet totally evaporates it cannot be activated again. The result in Figure 3c shows that the growth of the largest cloud droplet is similar to the control case, but the size of smallest cloud droplet also increases after each cycle. The reason for this CDS broadening is the Ostwald ripening effect, where large droplets grow at the expense of small ones. Past studies have concluded that the ripening effect is typically slow and inefficient for droplet growth (Wood et al., 2002). But the vertical oscillations near cloud base that are considered here allow for droplet deactivation and result the decrease of n with time (see Figure 3d), as in the control case. Thus, the typically inefficient Ostwald ripening is amplified through the

20

25

30

35



resulting deactivation of the smallest droplets. An early suggestion of this behavior is shown in Fig. 8 of Hagen (1979). The only difference between the control and this simulation is that n for the control case increases near the end of the simulation because of droplet reactivation (see Figure 3d). It should be mentioned that the step changes in n in Figure 3d are a result of using a discretized bin method to represent the continuous spectrum. A downward step in n means droplet deactivation, and an upwards step in n means droplet reactivation. Deactivation and reactivation can also be seen from the CDS D qualitatively: droplet deactivation occurs when the peak value of CDS D decreases (from red to blue as shown in Figure 2d), while droplet reactivation occurs when a subset of smaller cloud droplets appears.

From Figures 3 a and b, we can see that the solute effect contributes part of the CDS D broadening compared with the control case. But the solute effect alone is not enough to explain the growth of the largest cloud droplet. Droplet deactivation, which is related to the curvature effect, plays a crucial role here (see Figure 3c). Because the oscillations occur within the cloud region, 50 m above cloud base, droplet deactivation is surprising to us. There are two related questions: (1) Why and which droplet will deactivate? (2) Why is droplet deactivation related to the CDS D broadening?

The reason for the droplet deactivation is mainly because the cloud parcel experiences upwards and downwards oscillations. In the downdraft region, the air is subsaturated, which supports droplet evaporation. In addition, the saturated water vapor pressures over polydisperse droplets are different via both the solute and curvature effects. Smaller droplets with less solute and larger radii of curvature have higher saturated water vapor pressures, and thus evaporate faster than larger droplets in the downdraft region. Therefore, smaller droplets will evaporate first in the downdraft region.

The reason why droplet deactivation is related to the CDS D broadening can be explained in two ways. From the thermodynamic point of view, the liquid water mixing ratio is roughly a constant at a given height for each cycle (see Figure 2a). As the n decreases due to the droplet deactivation, we can expect that on average droplet size will be larger because the same amount of water will be redistributed on fewer cloud droplets. From the kinematic point of view, quasi-steady state supersaturation (s_{qs}) will become larger after each cycle due to droplet deactivation, as shown in Figure 2b. s_{qs} , the environmental supersaturation in quasi-steady state, is inversely proportional to the integral of mean droplet size \bar{r} and droplet number concentration (n), $s_{qs} \propto (\bar{r}n)^{-1}$ (Lamb and Verlinde, 2011). Here the decrease in n due to droplet deactivation is much greater than the change of \bar{r} ; therefore, s_{qs} will increase with decreasing n . This means that larger droplets grow even faster in the updraft region, and smaller droplets evaporate even faster in the downdraft region – beyond the solute effect alone. Conversely, an increase in s_{qs} will enhance droplet deactivation for smaller droplets, and it will also reinforce the growth of larger droplets in a positive feedback.

One question relevant to precipitation initiation is how fast can the largest cloud droplet grow in an oscillating parcel compared with droplets in an ascending-only parcel? The mean (yellow dashed line) and largest/smallest (upper/lower gray dashed lines) cloud droplets in an ascending-only cloud parcel are also shown in Figure 2d. It can be seen that the size of the largest



cloud droplet at cloud top in each cycle of the oscillating parcel (blue color bar) is similar to that in the ascending-only parcel (upper gray line). This is quite surprising because when the parcel reaches 1200 m for the first time (i.e., the top of the oscillation cycle), the largest cloud droplet radius is 9.07 μm (see Table 1 and Figure 2c); however after several cycles, the largest cloud droplet radius is 17.3 μm , still at 1200 m. The size is similar to the largest droplet size in an ascending-only parcel at a height of about 6000 m. This means that the largest cloud droplet size in an oscillating parcel at 1200 m is much larger than calculated from a traditional cloud parcel model (ascent only), and hence shows “superadiabatic” growth. It should be mentioned that cloud droplets in the ascending-only parcel at 6000 m are supercooled (around 248 K), but we ignore ice nucleation in this study. In addition, the size of the smallest cloud droplet and the mean droplet size are larger in an ascending-only parcel. Differences between the mean droplet sizes increases after each cycle, especially at the end of the simulation due to the reactivation of numerous small droplets. Therefore, the relative dispersion, which is the ratio of the standard deviation to the mean of a droplet size distribution, also increases after each cycle, and is much larger than in an ascending-only cloud parcel. Broadening of the CDS might quicken precipitation processes, and the increase of the relative dispersion is relevant to the albedo effect and increase albedo susceptibility (Feingold et al., 1997; Liu and Daum, 2002; Feingold and Siebert, 2009).

3.2 Sensitivity studies

In this subsection, we investigate effects of several factors on the CDS in the adiabatic parcel model with vertical oscillations. These factors include variations in the total aerosol number concentration, updraft velocity, and thickness of the recycling layer.

3.2.1 Effect of total aerosol number concentration

We test two other aerosol number concentrations by increasing and decreasing the number concentrations of the control by an order of magnitude, 10^2 cm^{-3} and 10^4 cm^{-3} , and keep the median radius and geometric standard deviation the same (see Figures 4 a and c). The results show that the CDS for the relatively clean case (10^2 cm^{-3}) behaves similarly to the solute effect alone (compare Figures 3b and 4b) – there is neither droplet deactivation nor reactivation. The CDS broadening is due to the ripening effect alone, which is not as efficient as when it is accompanied by deactivation as in the control case. For the relatively polluted case (10^4 cm^{-3}), both droplet deactivation and reactivation occur (see Figure 4d). The largest cloud droplet acts similarly as that in the control case, while the smallest cloud droplet is larger 1.5 h into the simulation but then begins to become smaller compared with the control case. We interpret these observations as follows. For the clean case, all aerosols are activated, and all droplets are able to grow to a relatively large size, making them unlikely to deactivate. However for polluted case, not all CCN are activated, there are therefore some smaller droplets that cannot grow very large and they will evaporate first in the downdraft region.



3.2.2 Effect of vertical velocity

The effect of vertical velocity on the CDS is investigated next. For a relative low velocity of $\pm 0.1 \text{ m s}^{-1}$, the cloud parcel only experiences one and a half cycles within three hours (see Figure 5a). The parcel reaches cloud base around 1 hour, significantly later than the control case due to the small velocity (see Figure 5a). However, the largest cloud droplet size ultimately becomes similar to that in the control case, and we also see the cloud droplet number concentration decrease due to droplet deactivation. No droplet reactivation occurs because the small velocity generates a low supersaturation in the updraft region, which is unfavorable for droplet reactivation. For a relative high velocity of $\pm 1.0 \text{ m s}^{-1}$, the cloud parcel can cycle more times within three hours (see Figure 5c). The parcel reaches cloud base faster than the control case (see Figure 5c). Both droplet deactivation and reactivation occur in this case, and the largest and smallest cloud droplets behave similarly to the control case.

10

3.2.3 Effect of the thickness of cycling layer

Two different cycling layers are also tested here. For a recycling layer of 150 m , which is 100 m thinner than the control case, the parcel experiences more cycles within three hours (see Figure 6a). The total cloud droplet number concentration decreases with time due to droplet deactivation, but no droplet reactivation occurs (see Figure 6b). Therefore the largest cloud droplet is similar to the control case, but the smaller cloud droplet is larger than the control case. For a cycling layer of 350 m , the parcel can penetrate the cloud base each cycle (see Figure 6c). In this case, all cloud droplets are deactivated below cloud base and reactivated again when the cloud parcel is supersaturated in the next ascending branch. Therefore the CDS is repeated and no broadening occurs.

20 3.3 Discussion

Table 1 summarizes the microphysical properties at cloud top for different cases. When the cloud parcel first reaches about 1200 m , the largest cloud droplet radius (r_{max}) is $9.07 \mu\text{m}$ (case 0). If the cloud parcel continues rising for three hours as for the ascending-only case, $r_{max} = 17.0 \mu\text{m}$ at 6000 m . However if the parcel experiences cycling within cloud region, r_{max} can also be around $17.0 \mu\text{m}$ as long as deactivation occurs, except for the low N_a case (see Table 1). In addition if reactivation also occurs, the relative dispersions are closer to observations, which are usually larger than 0.1 (Liu and Daum, 2002; Chandrakar et al., 2016).

From the above, we see that droplet deactivation and droplet reactivation play crucially important roles in CDS broadening in this study. Deactivation of smaller droplets is important for the growth of larger cloud droplets (e.g., see Figures 2d, 3c, 4d, 5b,d and 6b). Droplet deactivation occurs in the descending branch for smaller droplets due to both the curvature and solute effects (Ostwald ripening). The evaporation of smaller cloud droplets with less solute makes water vapor available for the

30



growth of other larger cloud droplets. On average, the largest cloud droplet size increases with time after each cycle.

One interesting result is that the size of the largest cloud droplet within each cycle is similar to that in the ascending-only parcel (i.e., approximately within one micrometer), as shown in Figure 7. The general trends approximately follow a linear mass growth rate that is independent of aerosol number concentration, vertical velocity and the thickness of the oscillation layer, as long as deactivation occurs. This suggests that the growth of the largest cloud droplets strongly depends on the amount of time such droplets remain in the cloud, rather than the temporal variability of supersaturation in updrafts and downdrafts. The reason is that the environmental (i.e., the in-cloud) saturation ratio (S_e) is buffered by the equilibrium saturation ratio (S_{sat}) over smaller droplets. Figure 8 shows the changes of S_e and S_{sat} over two droplets (same used as in Figure 2c) in the control case. Instead of being symmetric around 1 for the pure water case (ignoring solute and curvature effects), S_e in the oscillating parcel is symmetric around S_{sat} over the small cloud droplets. For example before 1.5 hours, droplets formed on $r_a = 51\text{ nm}$ are the smallest cloud droplets in the population, and the average S_e (gray line) during one oscillation is roughly symmetric around the blue line (Figure 8). The fact that S_e is buffered by S_{sat} over small cloud droplets is mainly because the number concentration of the smallest cloud droplet (36 cm^{-3} in the control case) is much larger than that of large cloud droplet ($1.8 \times 10^{-9}\text{ cm}^{-3}$). When those small droplets totally evaporate (between 1.5 to 2.5 hours), S_{sat} (blue line) for those deactivated droplets is the same as S_e (gray line). During this period, S_e is symmetric around S_{sat} over the remaining small droplets (larger than the droplets formed on $r_a = 51\text{ nm}$ but smaller than for $r_a = 503\text{ nm}$). When the droplets formed on $r_a = 51\text{ nm}$ are reactivated (after 2.5 hours), S_e is symmetric around $S_{sat}(r_a = 51\text{ nm})$ again until they are deactivated. It should be mentioned that number concentration of those reactivated droplets increases steady after each cycle after 2.0 hours (See Figure 3d). By the end of the simulation, the number concentration of the reactivated droplets is similar to that of the remaining large droplets (about 150 cm^{-3}). Therefore, the effect of those reactivated droplets on the environmental saturation ratio becomes stronger after 2.0 hours (see Figure 8).

This symmetric property of S_e can be also explained using the quasi-steady supersaturation s_{qs} . For pure water droplets, $s_{qs} \sim \frac{w}{nr}$ (Lamb and Verlinde, 2011). A symmetric distribution of w around 0 will generate a symmetric distribution of s_{qs} around 0 (i.e., S_e around 1). If the curvature and solute effects are considered, s_{qs} will be symmetric around s_k given the same condition of w , because $s_{qs} \sim \frac{w}{nr} + s_k$, where $s_k = S_{sat} - 1$ is the equilibrium supersaturation ratio over a mono-disperse droplet. For polydisperse cloud droplets, the environment conditions are buffered by the large number of small cloud droplets. Therefore S_e is symmetric around S_{sat} over smaller droplets before they totally evaporate in the oscillating parcel. $\overline{S_e} - S_{sat}$ controls the growth of a large droplet and it is positive on average. That is why the large droplets can grow after each cycle. In addition, the influence of S_e fluctuations on droplet growth is small if S_{sat} over a large droplet is much lower than S_e and its fluctuations. The extreme examples of this phenomenon are when droplets form on GCCN in warm clouds (Jensen and Nugent, 2017) or ice particles form in mixed phase clouds. Therefore, the growth of the large droplet here is dominated by its in-cloud lifetime.



5 However if all cloud droplets are deactivated, CDSB broadening does not occur (see Figure 6d). Without droplet deactivation, the CDSB can also broaden due just to the solute effect, as is the case when the curvature effect is ignored (Figure 3b) or when the total aerosol number concentration is low (Figure 4b). CDSB broadening due to the ripening effect without droplet deactivation is not as significant as it is with droplet deactivation, but it also might be important after several hours as suggested by Wood et al. (2002).

10 Droplet reactivation usually occurs in the updraft region after several cycles, and those reactivated droplets will be deactivated again in the downdraft region. Formation of smaller cloud droplets can broaden the CDSB at smaller sizes, decrease the mean cloud droplet size, and increase the relative dispersion. Meanwhile, the generation of new cloud droplets also suppresses the growth of larger cloud droplets (see Figure 2d).

4 Conclusions and atmospheric implications

15 In this study, we investigate the condensation growth of cloud droplets in an adiabatic parcel with vertical oscillations based on a Lagrangian bin-microphysics cloud parcel model where cloud droplets are formed on polydisperse, sub-micrometer aerosol particles. Both the solute and curvature effects are considered for all cloud droplets before and after activation during the whole simulation. The CDSB can also broaden by condensation growth due to Ostwald ripening together with droplet deactivation and reactivation, which is consistent with the results of Korolev (1995). Droplet deactivation occurs in the descending branch due to the combination of the solute and curvature effects. Deactivation of smaller droplets makes water vapor available for other larger droplets, and thus broadens the CDSB at larger sizes. The growth of the largest cloud droplet approximately follows a linear mass growth rate after each cycle, and it is independent of aerosol number concentration, vertical velocity, and the thickness of the oscillation layer, as long as deactivation occurs. The size of the largest cloud droplet strongly depends on the time that droplet remains in the cloud rather than on the variability of the in-cloud supersaturation. This is because the environmental air is buffered by the large number of smaller cloud droplets: the environmental saturation ratio in an oscillating parcel is symmetric around the equilibrium saturation ratio over smaller cloud droplets. The linear mass growth rate can be used to roughly estimate the right upper boundary of the CDSB, at least in this study. Droplet reactivation usually occurs after a few cycles. These cloud droplets are activated in the ascending branch, and deactivated in the descending branch. They are usually very small (less than $5 \mu\text{m}$) and thus broaden the CDSB at smaller sizes. The mean cloud droplet size significantly decreases when reactivation occurs, which leads to an increase in relative dispersion. On the other hand, those newly-formed cloud droplets compete against other cloud droplets for water vapor, thus suppressing the growth of larger cloud droplets.

30

We note that there are additional factors that might affect droplet growth that are not treated in this study. For example, we do not consider the sedimentation of cloud droplets in this study, similar to Korolev et al. (2013) and Jensen and Nugent (2017). This is a reasonable assumption for an updraft velocity of 0.5 m s^{-1} or above, but ignoring sedimentation in the low velocity



case (0.1 m s^{-1}) will limit the accuracy of our results. Entrainment and mixing are also ignored here. In addition, we do not consider the collision coalescence between droplets. Although CDSB broadening is favorable for collision processes, it might be interesting to determine how this broadening will accelerate rain formation.

5 We have used idealized simulations to find this new CDSB broadening mechanism, so it is reasonable to ask if this mechanism is likely to occur in nature. To answer this question, we investigate the two necessary conditions for this mechanism and address whether these conditions exist in real clouds. The first necessary condition is that droplets form on polydisperse aerosol particles with different solute effects. This is a very general occurrence in the atmosphere due to the complexity of aerosol size and composition. The second necessary condition is that a cloud experiences upward and downward oscillations. This is also
10 a general occurrence in natural clouds due to turbulence and circulations that can become established within a cloud layer. Therefore we expect that this mechanism of CDSB broadening is possible in the real clouds. How important this mechanism is to CDSB broadening in real clouds compared with other mechanisms is worth future investigation, but is beyond the scope of this study.

15 There is an implication of this mechanism for the cloud modeling community. Most of the bulk and bin microphysical schemes only consider the curvature and solute effects during the activation process based on Köhler theory. Cloud droplets are assumed to be pure water after they are activated. Tracking the solute distribution for each bin of cloud droplet is possible, but very computationally expensive (e.g., Bott, 2001; Lebo and Seinfeld, 2011). The mechanism of CDSB broadening in this study requires the model to consider both solute and curvature effects before and after activation. Large eddy simulations with
20 a similar microphysical treatment would be useful to investigate how important this mechanism is to CDSB broadening in more realistic clouds.

Acknowledgements. F.Y., P.K. and A.M.V. were supported by the U.S. Department of Energy (DOE) under Contract DE-SC0012704. R.A.S. was supported by the DOE Office of Science as part of the Atmospheric System Research program through grant no. DE-SC0011690.



References

- Bott, A.: A new method for the solution of the stochastic collection equation in cloud models with spectral aerosol and cloud drop micro-physics, *Atmospheric research*, 59, 361–372, 2001.
- Boucher, O., Randall, D., Artaxo, P., Bretherton, C., Feingold, G., Forster, P., Kerminen, V.-M., Kondo, Y., Liao, H., Lohmann, U., et al.:
5 Clouds and aerosols, in: *Climate change 2013: the physical science basis. Contribution of Working Group I to the Fifth Assessment Report of the Intergovernmental Panel on Climate Change*, pp. 571–657, Cambridge University Press, 2013.
- Chandrakar, K. K., Cantrell, W., Chang, K., Ciochetto, D., Niedermeier, D., Ovchinnikov, M., Shaw, R. A., and Yang, F.: Aerosol indirect effect from turbulence-induced broadening of cloud-droplet size distributions, *Proceedings of the National Academy of Sciences*, 113, 14 243–14 248, 2016.
- 10 Cheng, W. Y., Carrió, G. G., Cotton, W. R., and Saleeby, S. M.: Influence of cloud condensation and giant cloud condensation nuclei on the development of precipitating trade wind cumuli in a large eddy simulation, *Journal of Geophysical Research: Atmospheres*, 114, 2009.
- Cooper, W. A., Lasher-Trapp, S. G., and Blyth, A. M.: The influence of entrainment and mixing on the initial formation of rain in a warm cumulus cloud, *Journal of the Atmospheric Sciences*, 70, 1727–1743, 2013.
- Ervens, B. and Feingold, G.: On the representation of immersion and condensation freezing in cloud models using different nucleation
15 schemes, *Atmospheric Chemistry and Physics*, 12, 5807–5826, 2012.
- Falkovich, G. and Pumir, A.: Sling effect in collisions of water droplets in turbulent clouds, *Journal of the Atmospheric Sciences*, 72, 2015.
- Feingold, G. and Kreidenweis, S.: Does cloud processing of aerosol enhance droplet concentrations?, *Journal of Geophysical Research: Atmospheres*, 105, 24 351–24 361, 2000.
- Feingold, G. and Siebert, H.: *Cloud-aerosol interactions from the micro to the cloud scale*, 2009.
- 20 Feingold, G., Boers, R., Stevens, B., and Cotton, W. R.: A modeling study of the effect of drizzle on cloud optical depth and susceptibility, *Journal of Geophysical Research: Atmospheres*, 102, 13 527–13 534, 1997.
- Feingold, G., Walko, R., Stevens, B., and Cotton, W.: Simulations of marine stratocumulus using a new microphysical parameterization scheme, *Atmospheric research*, 47, 505–528, 1998.
- Feingold, G., Cotton, W. R., Kreidenweis, S. M., and Davis, J. T.: The impact of giant cloud condensation nuclei on drizzle formation in
25 stratocumulus: Implications for cloud radiative properties, *Journal of the atmospheric sciences*, 56, 4100–4117, 1999.
- Göke, S., Ochs III, H. T., and Rauber, R. M.: Radar analysis of precipitation initiation in maritime versus continental clouds near the Florida coast: Inferences concerning the role of CCN and giant nuclei, *Journal of the Atmospheric Sciences*, 64, 3695–3707, 2007.
- Grabowski, W. W. and Wang, L.-P.: Growth of cloud droplets in a turbulent environment, *Annual Review of Fluid Mechanics*, 45, 293–324, 2013.
- 30 Hagen, D. E.: A numerical cloud model for the support of laboratory experimentation, *Journal of Applied Meteorology*, 18, 1035–1043, 1979.
- Heintzenberg, J., Charlson, R. J., Brenguier, J.-L., Haywood, J., Nakajima, T., and Stevens, B.: Clouds in the perturbed climate system: Part2 Particle hygroscopicity and cloud condensation nucleus activity, *Their rela*, 2009.
- Hocking, L.: The collision efficiency of small drops, *Quarterly Journal of the Royal Meteorological Society*, 85, 44–50, 1959.
- 35 Jensen, J. B. and Lee, S.: Giant sea-salt aerosols and warm rain formation in marine stratocumulus, *Journal of the atmospheric sciences*, 65, 3678–3694, 2008.



- Jensen, J. B. and Nugent, A. D.: Condensational growth of drops formed on giant sea-salt aerosol particles, *Journal of the Atmospheric Sciences*, 74, 679–697, 2017.
- Korolev, A., Pinsky, M., and Khain, A.: A new mechanism of droplet size distribution broadening during diffusional growth, *Journal of the Atmospheric Sciences*, 70, 2051–2071, 2013.
- 5 Korolev, A. V.: The influence of supersaturation fluctuations on droplet size spectra formation, *Journal of the atmospheric sciences*, 52, 3620–3634, 1995.
- Kostinski, A. B. and Shaw, R. A.: Fluctuations and luck in droplet growth by coalescence, *Bulletin of the American Meteorological Society*, 86, 235–244, 2005.
- Laird, N. F., Ochs Iii, H. T., Rauber, R. M., and Miller, L. J.: Initial precipitation formation in warm Florida cumulus, *Journal of the atmospheric sciences*, 57, 3740–3751, 2000.
- 10 Lamb, D. and Verlinde, J.: *Physics and chemistry of clouds*, Cambridge University Press, 2011.
- Lasher-Trapp, S. G., Cooper, W. A., and Blyth, A. M.: Broadening of droplet size distributions from entrainment and mixing in a cumulus cloud, *Quarterly Journal of the Royal Meteorological Society*, 131, 195–220, 2005.
- Lebo, Z. and Seinfeld, J.: A continuous spectral aerosol-droplet microphysics model, *Atmospheric Chemistry and Physics*, 11, 12 297–12 316, 15 2011.
- Li, Z., Xue, H., and Yang, F.: A modeling study of ice formation affected by aerosols, *Journal of Geophysical Research: Atmospheres*, 118, 2013.
- Liu, Y. and Daum, P. H.: Anthropogenic aerosols: Indirect warming effect from dispersion forcing, *Nature*, 419, 580–581, 2002.
- Low, R. D.: A generalized equation for the solution effect in droplet growth, *Journal of the Atmospheric Sciences*, 26, 608–611, 1969.
- 20 Lozar, A. d. and Muessle, L.: Long-resident droplets at the stratocumulus top, *Atmospheric Chemistry and Physics*, 16, 6563–6576, 2016.
- Lu, J. and Shaw, R. A.: Charged particle dynamics in turbulence: Theory and direct numerical simulations, *Physics of Fluids*, 27, 065 111, 2015.
- Mordy, W.: Computations of the growth by condensation of a population of cloud droplets, *Tellus*, 11, 16–44, 1959.
- Naumann, A. K. and Seifert, A.: A Lagrangian drop model to study warm rain microphysical processes in shallow cumulus, *Journal of Advances in Modeling Earth Systems*, 7, 1136–1154, 2015.
- 25 Paluch, I. R.: Theoretical collision efficiencies of charged cloud droplets, *Journal of Geophysical Research*, 75, 1633–1640, 1970.
- Pruppacher, H. R., Klett, J. D., and Wang, P. K.: *Microphysics of clouds and precipitation*, 1998.
- Siebert, H. and Shaw, R. A.: Supersaturation fluctuations during the early stage of cumulus formation, *Journal of the Atmospheric Sciences*, 74, 975–988, 2017.
- 30 Wood, R., Irons, S., and Jonas, P.: How important is the spectral ripening effect in stratiform boundary layer clouds? Studies using simple trajectory analysis, *Journal of the atmospheric sciences*, 59, 2681–2693, 2002.
- Xue, H. and Feingold, G.: A modeling study of the effect of nitric acid on cloud properties, *Journal of Geophysical Research: Atmospheres*, 109, 2004.
- Yang, F., Xue, H., Deng, Z., Zhao, C., and Zhang, Q.: A closure study of cloud condensation nuclei in the North China Plain using droplet kinetic condensational growth model, *Atmospheric Chemistry and Physics*, 12, 5399–5411, 2012.
- 35 Yang, F., Shaw, R., and Xue, H.: Conditions for super-adiabatic droplet growth after entrainment mixing, *Atmospheric Chemistry and Physics*, 16, 9421–9433, 2016.



Yin, Y., Levin, Z., Reisin, T. G., and Tzivion, S.: The effects of giant cloud condensation nuclei on the development of precipitation in convective clouds—A numerical study, *Atmospheric research*, 53, 91–116, 2000.



Table 1. Microphysical properties at cloud top for different cases: r_{max} is the largest cloud droplet radius, r_{min} is the smallest cloud droplet radius, \bar{r} is the mean cloud droplet size, σ is the standard deviation of droplet radius, and σ/\bar{r} is the relative dispersion. Case 0 is when the cloud parcel reaches the cloud top for the first time with the same setup as the control case (shown as black circle in Figure 3). For other cases, results represent the parcel at cloud top for the last time after 3 hours simulation; the example of the control case is shown as the green circle in Figure 3.

	r_{max} (μm)	r_{min} (μm)	\bar{r} (μm)	σ (μm)	$\frac{\sigma}{\bar{r}}$	deactivation	reactivation
case 0	9.07	4.15	5.82	0.51	0.088	no	no
ascending only	17.0	11.5	13.3	0.55	0.041	no	no
control	17.3	6.09	7.51	1.64	0.22	yes	yes
pure water	7.83	5.86	5.96	0.086	0.014	no	no
only solute effect	12.7	5.84	6.04	0.21	0.035	no	no
without reactivation	17.8	7.86	10.3	1.11	0.11	yes	no
low N_a	16.2	9.63	11.1	0.40	0.036	no	no
high N_a	16.8	3.05	4.65	1.48	0.32	yes	yes
low w	13.3	7.73	8.79	0.60	0.068	yes	no
high w	17.1	4.64	5.31	0.99	0.19	yes	yes
thin ΔH	17.0	6.15	8.53	1.40	0.16	yes	yes
thick ΔH	9.01	4.14	5.76	0.50	0.087	no	yes

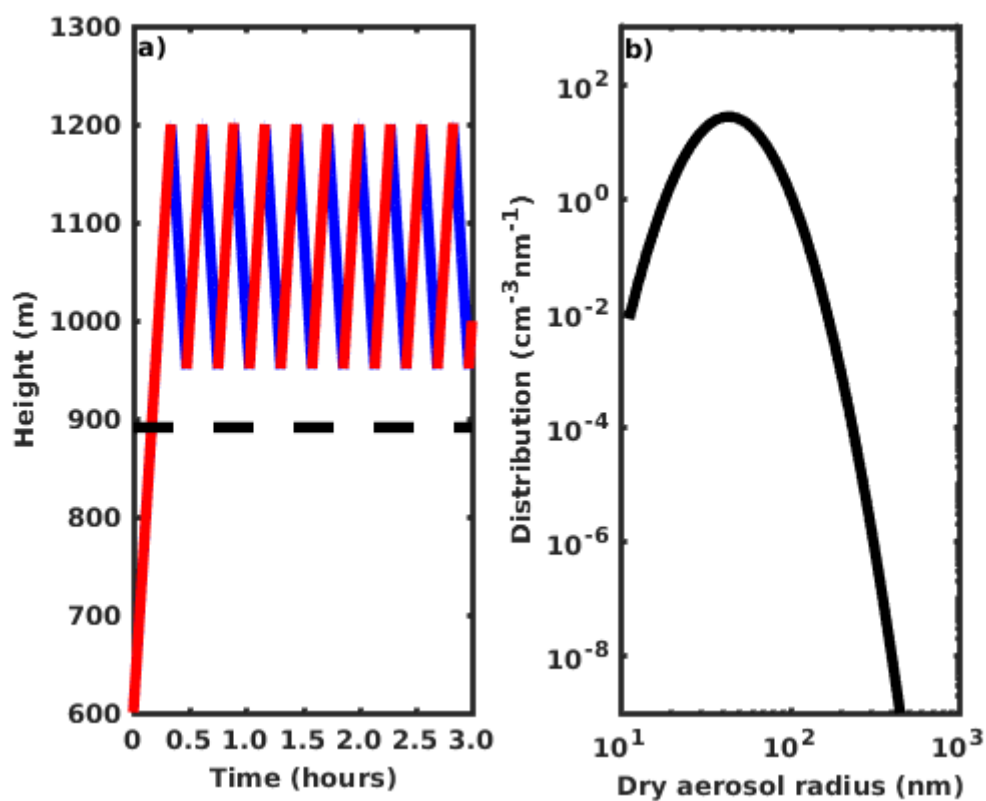


Figure 1. a) Trajectory of cloud parcel with upward and downward oscillations. Velocity is constant and is 0.5 m s^{-1} for the ascending parcel and -0.5 m s^{-1} for the descending parcel. The dashed line is the cloud base, and the red and blue lines represent ascending and descending parcels. b) Initial dry aerosol size distribution. The total aerosol number concentration is 1000 cm^{-3} .

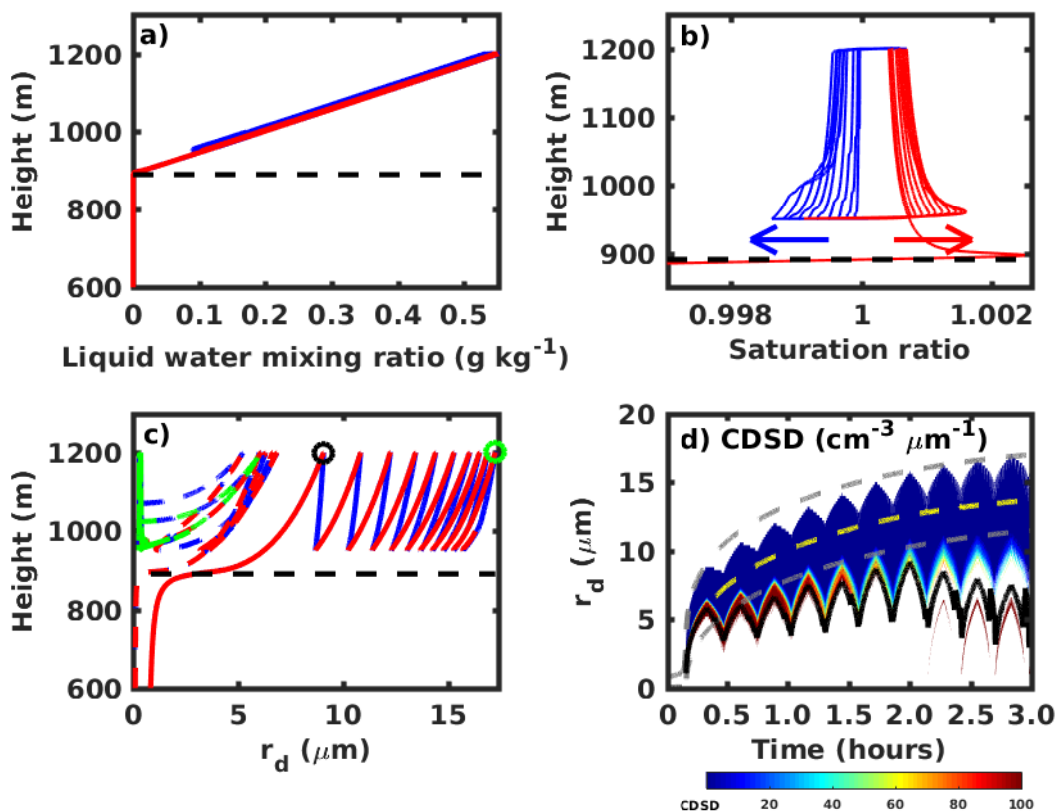


Figure 2. Thermodynamical and microphysical properties of an adiabatic cloud parcel with upward and downward oscillations. a) Liquid water mixing ratio changes with height. b) Cloud parcel saturation ratio changes with height. Arrows in b represent the evolution of saturation ratio profile with time. c) Radii changes of two selected cloud droplets with height. The solid line is for the largest cloud droplet that formed on a dry aerosol with radius of 503 nm, and the dashed line is for droplet that formed on an aerosol of 51 nm. The red and blue lines in a-c represent ascending and descending parcels, and the black dashed line indicates cloud base height. The green dashed line indicates the reactivation of that bin. The black and green circles are referred to in the text. d) Cloud droplet size distribution changes with time. The black line represents the mean cloud droplet radius change with time. The yellow dashed line is the change in mean droplet size for the ascending-only cloud parcel with a constant velocity of 0.5 m s^{-1} , and the upper and lower dashed gray lines represent the largest and smallest cloud droplets in the ascending-only parcel.

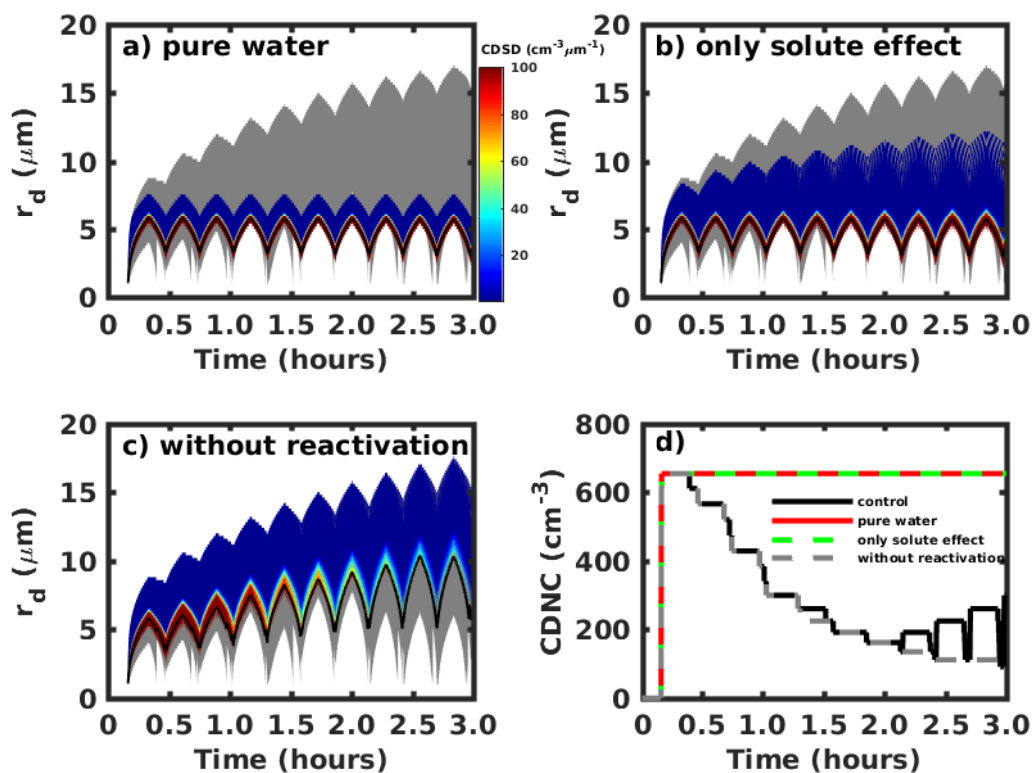


Figure 3. a) Cloud droplet size distribution (CDS) changes with time without solute or curvature effects. b) CDSC changes with time with the solute effect but without the curvature effect. c) CDS changes with time including both solute and curvature effects but where droplet reactivation is not considered. d) Total cloud droplet number concentration (n) changes with time for the different cases. The gray region in a-c represents the range of the droplet size spectrum for the control case, and the black lines represents the mean cloud droplet radius change with time.

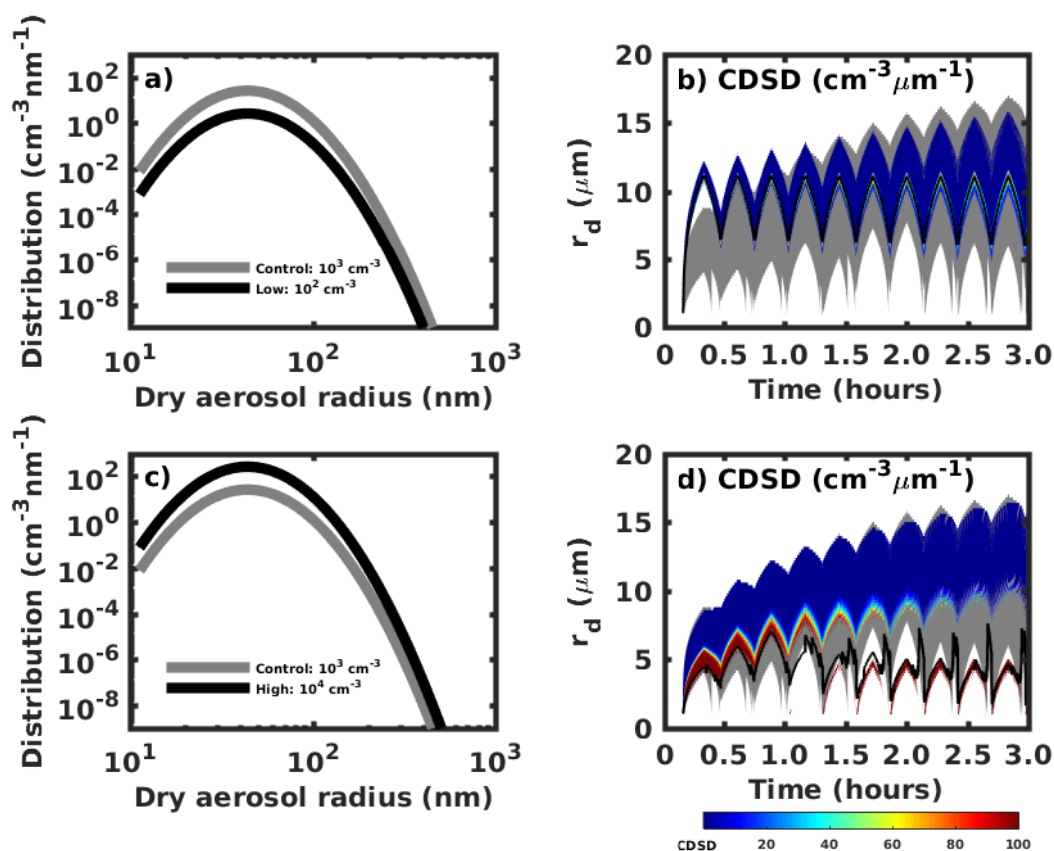


Figure 4. a) Aerosol size distribution for a low number concentration of 10^2 cm^{-3} . b) Cloud droplet size distribution changes with time for the low aerosol number concentration case. c) Aerosol size distribution for the high number concentration of 10^4 cm^{-3} . d) Cloud droplet size distribution changes with time for the high aerosol number concentration case. Gray lines in a and c represent the control case with a total aerosol number concentration of 10^3 cm^{-3} , and gray regions in b and d are the range of the cloud droplet size spectrum for the control case.

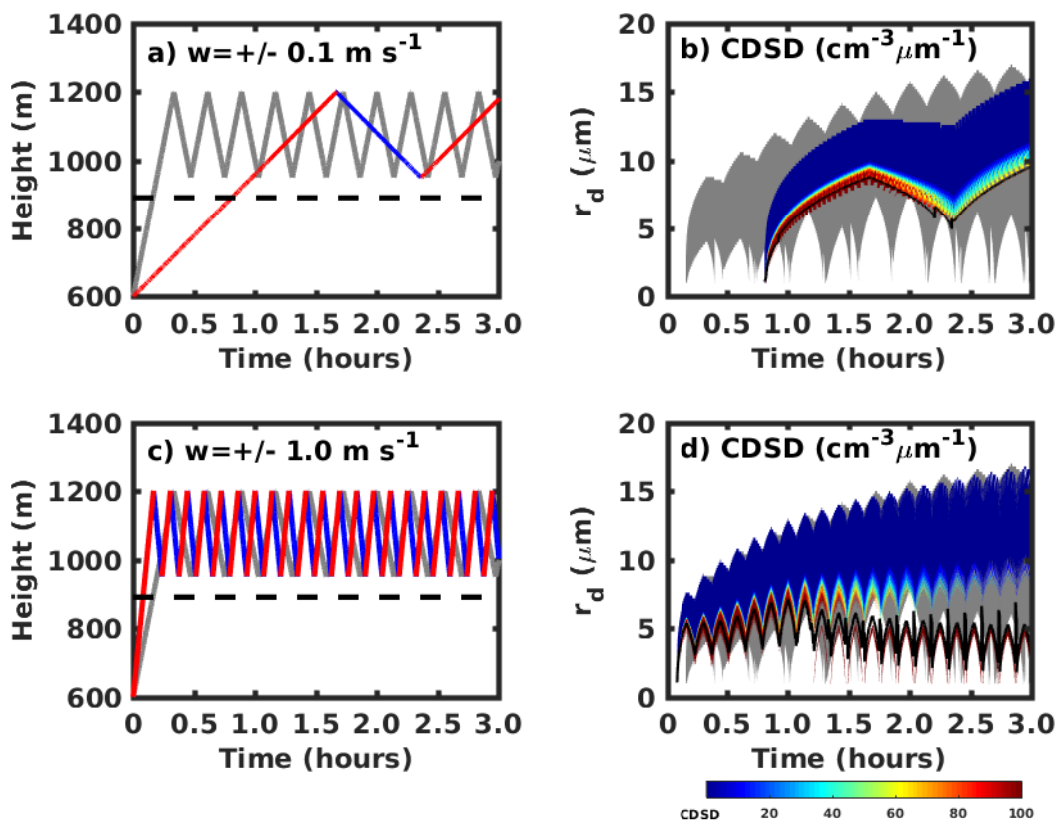


Figure 5. a) The height of cloud parcel changes with time for the low velocity case of $\pm 0.1 \text{ m s}^{-1}$. b) Cloud droplet size distribution changes with time for the low velocity case. c) The height of the cloud parcel changes with time for the velocity of $\pm 1.0 \text{ m s}^{-1}$. d) Cloud droplet size distribution changes with time for the high velocity case. Gray lines in a and c represent the control case with velocity of $\pm 0.5 \text{ m s}^{-1}$, and the gray regions in b and d are the range of cloud droplet spectrum for the control case.

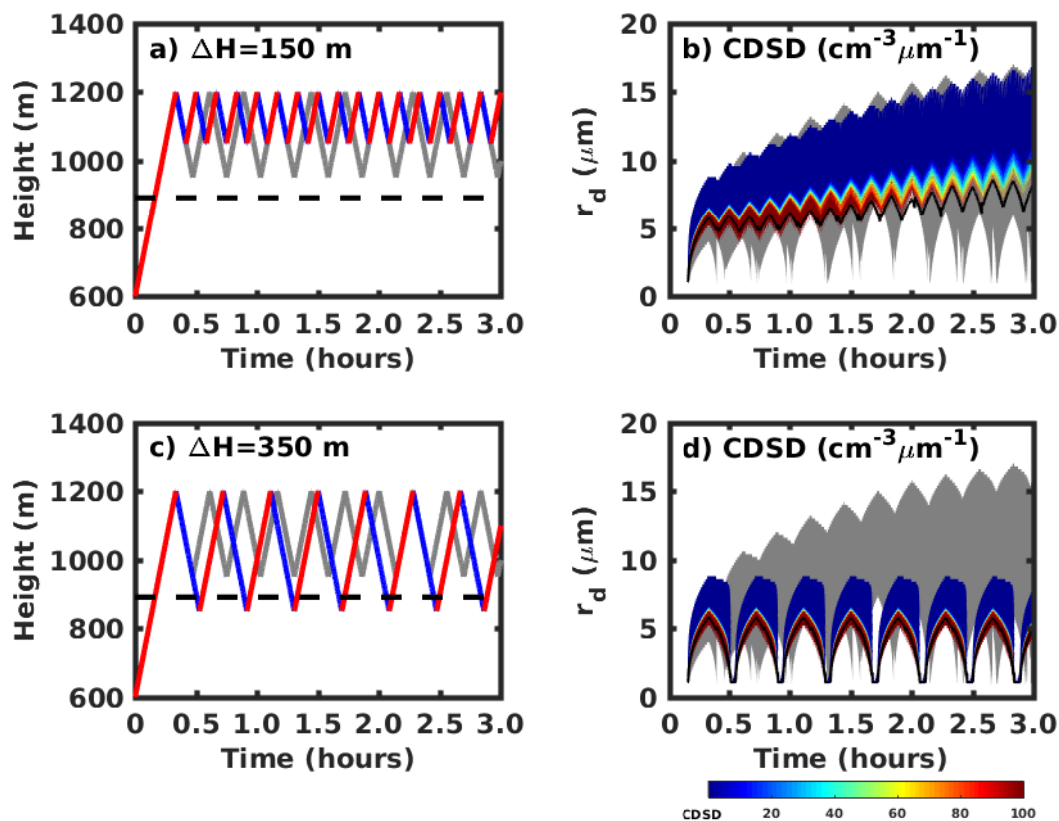


Figure 6. a) The height of cloud parcel changes with time for the thin cycling layer of 150 m. b) Cloud droplet size distribution changes with time for the thin cycling layer case. c) Aerosol size distribution for the thick cycling layer of 350 m. d) Cloud droplet size distribution changes with time for the thick cycling layer case. The gray lines in a and c represent the control case with cycling layer of 250 m, and the gray regions in b and d are the range of cloud droplet size spectrum for the control case.

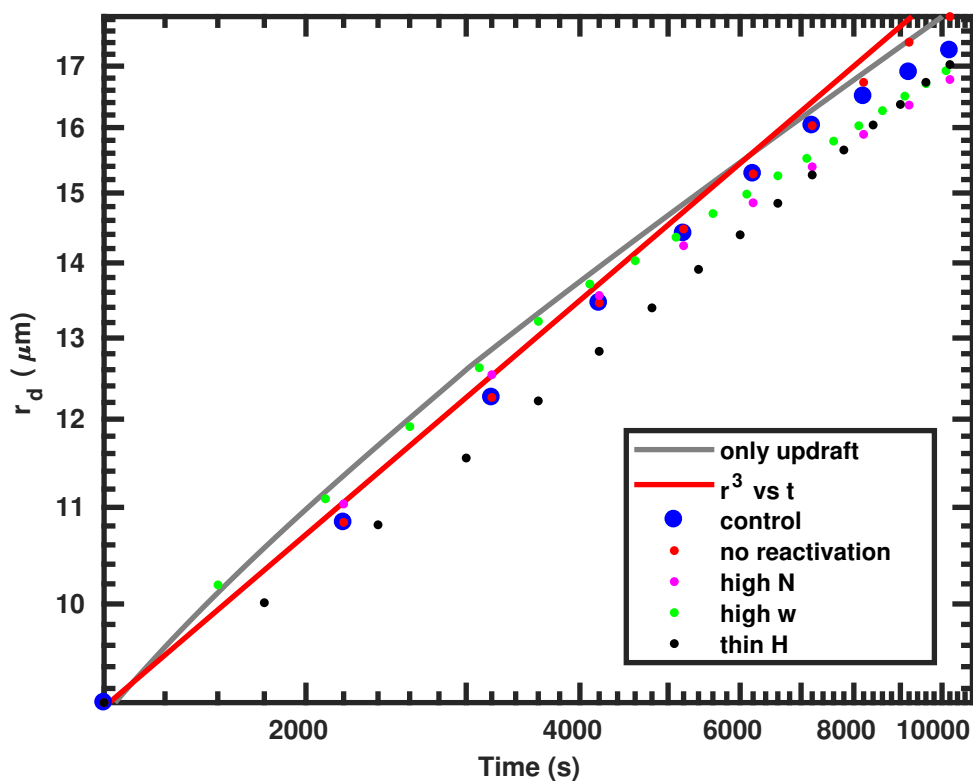


Figure 7. The largest cloud droplet size after each cycle is plotted for different cases discussed before: blue dots, control case; red dots, no reactivation case; pink dots, high number concentration case; green dots, high vertical velocity case; and black, thin oscillation layer case. The gray line is for the ascending-only case from Figure 4, and the red line represents the growth of a droplet with a linear mass growth rate.

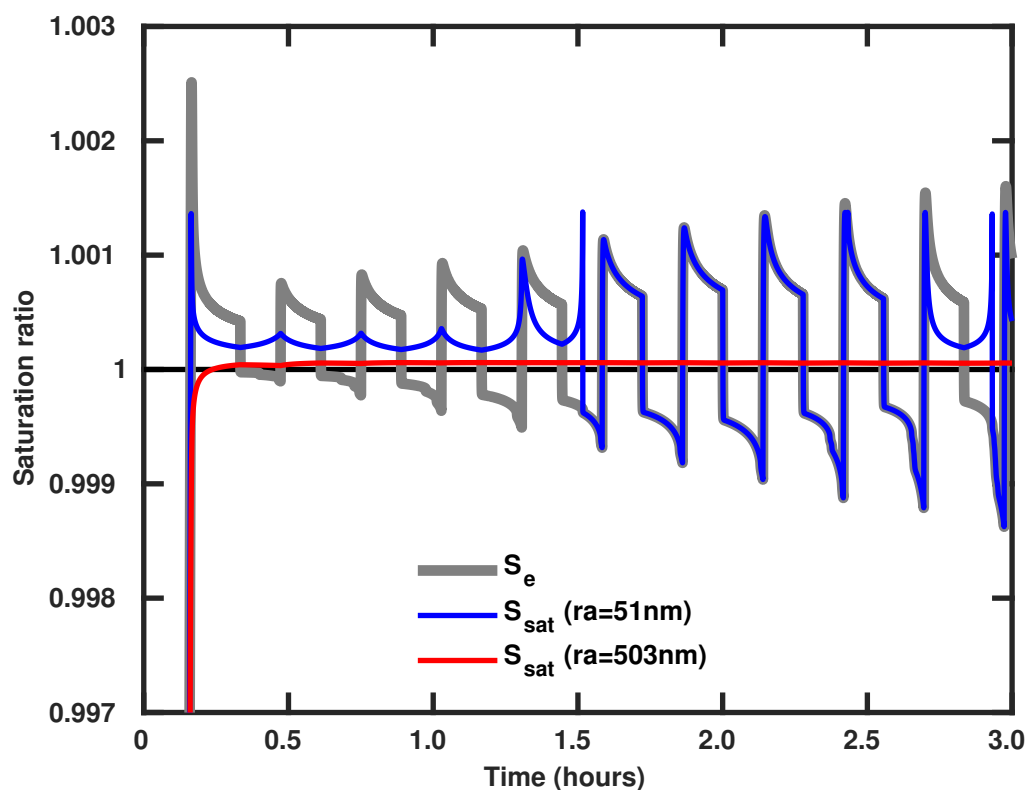


Figure 8. Changes of environmental saturation ratio (grey) and equilibrium saturation ratios over two droplets (red and blue) with time in an oscillating parcel. The blue line is for a droplet formed on a dry aerosol with radius of 53 nm and the red line is for a droplet formed on a dry aerosol with radius of 503 nm . The smaller cloud droplet (formed on a dry aerosol with radius of 53 nm) deactivates at approximately 1.5 hours and reactivates at approximately 2.5 hours.